Dynamic Buffer Status based Control for LTE-A Network with Underlay D2D Communication

Alia Asheralieva and Yoshikazu Miyanaga, *Senior Member, IEEE*

***Abstract*—This paper explores the problem of joint mode selection, spectrum management, power control and interference mitigation for device-to-device (D2D) communication underlaying a Long Term Evolution Advanced (LTE-A) network. We consider a dynamic mode selection scenario, in which the modes (D2D or cellular) of the devices depend on optimal allocations. To improve the quality of service (QoS) for the users, the optimization objective in a corresponding problem is formulated in terms of buffer size of user equipments (UEs), which is estimated based on buffer status information collected by the UEs. The realizations of a resource allocation approach presented in the paper include its real-time and non-real-time implementations, as well as two modifications applicable to a standard LTE-Direct (LTE-D) network. Performance of the proposed algorithms has been evaluated using the OPNET-based simulations. All algorithms show improved performance in terms of mean packet end-to-end delay when compared to most relevant schemes proposed earlier.**

***Index Terms*—Device-to-Device communication, LTE, LTE-Advanced, LTE-Direct, resource allocation.**

I. Introduction

D2D communication has been proposed to increase spectral efficiency of the network by allowing direct communication between two mobile users without traversing the Base Station (BS) or core network [1], [2]. In underlay D2D communication, the D2D users can reuse cellular spectrum, and communicate directly while remaining controlled by the BS. Note that both cellular users (CUs) and D2D users (DUs) share the same radio resources, and therefore it is essential to control the interference caused by CUs to DUs, and vice versa [2].

Adequate interference management for D2D communication can significantly improve performance of cellular networks (in terms of spectrum efficiency, cellular coverage, overall network throughput, user experience, etc.). Although the objectives here could be different, to achieve the optimal system performance such problems as D2D/cellular mode selection, spectrum assignment, power control, and interference mitigation should be considered jointly when designing the algorithm. Related references in this area are [3] – [8], studying the problem of interference mitigation for underlaying D2D communication. It should be noted, however, that the majority of the proposed formulations do not deal with the issues of D2D/cellular mode selection, spectrum assignment and interference management in a joint fashion, but rather by splitting the original problem into smaller sub-problems (see, e.g., [7]), or by separating the time scales of these sub-problems ([6]). Hence, although the complexity of such methods is less than the complexity of an algorithm with joint resource allocation, their efficiency in terms of maximizing some certain optimality criteria is clearly downscaled.

In addition, many of the existing resource allocation techniques focus on supporting the physical (PHY) layer service quality (measured in terms of the number of PHY connections, signal-to-interference and noise ratio (SINR), PHY-layer throughput, spectrum and power efficiency, etc.). However, the designs optimized for PHY throughput are not automatically good for providing the higher-layer QoS. Therefore, it is impossible to evaluate the actual performance of these methods for end-to-end applications.

The main contributions of this work are the following. We consider a dynamic mode selection scenario, in which the modes (D2D or cellular) of the devices are adjusted according to optimal allocations. The corresponding problem is formulated as the joint mode, spectrum and power allocation problem with the objective to minimize the maximal buffer size of UEs subject to target interference constraints. It should be noted that the size of UE's buffer is directly related to the packet end-to-end delay and loss (which determine the user-perceived QoS) and can be readily estimated based on buffer status information collected by user devices and sent to the evolved NodeB (eNB) within the LTE packet scheduling procedure [11].

According to the conveyed literature review, there are no prior works on delay-aware D2D networking. However, many research contributions have been presented in a more general area of delay-aware wireless networks (e.g., [12] - [14]). Existing approaches to reduce the end-to-end latency in wireless networks are [12]:

- large derivation: a simple channel state information (CSI) based policy which results in good delay performance only for a large delay regime;
- Lyapunov drift: a simple throughput optimal policy that provides a weak form of delay performance based on stability;
- stochastic majorization: the longest-queue-highest-possible rate policy, which is delay-optimal only for the cases with symmetric and homogeneous users;
- Markov decision process (MDP): a brute-force value iteration which is complex with the curse of dimensionality.

Clearly, all of the above methods have both the strong points and disadvantages. The approach used in this paper can be regarded as a form of stochastic majorization, which is not as complex as MDP, but shows much better results (in terms of achieved delay performance) than large derivation and Lyapunov drift methods.

To reduce the complexity of the proposed resource allocation schemes, a modification of the Alternating Direction Method of Multipliers (ADMM) [15] is used in this paper. This method decomposes a large problem into a number of small easily solvable sub-problems, and therefore can be run on parallel computers to reduce the solution time. The ADMM algorithm was originally introduced in early 1970s [16], and has since been studied extensively (e.g., [17] – [22]). Recently, it has become popular in various engineering fields involving large-scale data, mainly due to its decomposition ability and its convergence guarantees on a wide range of problems [15].

The rest of the paper is organized as follows. A general network model (including mode selection, spectrum usage and channel model) is described in Section II. Resource allocation problem is formulated in Section III. The algorithm for resource allocation is presented in Section IV. The algorithm implementation in LTE-A network is discussed in Section V. Simulation model and performance evaluation of the algorithms is given in Section VI. Results of this work are summarized in Conclusion.

II. Network Model

In this paper, the problem of resource allocation for D2D communication is investigated for both the uplink (UL) and the downlink (DL) directions. Similarly, the discussion through the rest of the paper is applicable (if not stated otherwise) to either direction. Consider a basic LTE-A network which consists of one eNBs and N UEs numbered $U_1, \ldots, U_N$. Let $\mathbf{N} = \{1, \ldots, N\}$ be the set of the all users' indices in the network. Note, that in LTE system, the unique users' identification numbers (IDs) can be found from the standard random access channel (RACH) procedure, which is used for initial access to the network (i.e., for originating, terminating or registration call) [23], [24]. Described network operates on a slotted-time basis with the time axis partitioned into equal non-overlapping time intervals (slots) of the length T_s, with t denoting an integer-valued slot index.

A. Mode Selection

The user devices in the considered model operate either in a traditional cellular mode or in D2D mode. The DUs access the network resources using an underlay D2D model, where each CU may share its frequency band with one or more DUs. In LTE-A, the respective IDs of CUs/DUs can be determined from a standard session initiation protocol (SIP) procedure which is used to setup user sessions. A detailed description of the SIP procedure and its use for D2D access is given in [25]. Correspondingly, it is possible to form two sets: set $\mathbf{C}$ containing the indices of the users which can operate only in cellular mode, and set $\mathbf{D}$ containing the indices of potential D2D users. Clearly, $\mathbf{C} \cap \mathbf{D} = \emptyset$ and $\mathbf{C} \cup \mathbf{D} = \mathbf{N}$. Note, that the sets $\mathbf{C}$ and $\mathbf{D}$ can be specified based on, e.g., the proximity[1] of the users to each other and/or type of user application (e.g., video sharing, gaming, proximity-aware social networking). Such information can be acquired from the standard session initiation protocol (SIP) procedure which is used to setup user sessions (detailed description of the SIP and its use for D2D access can be found in [24]) or upon user arrival to the network (i.e., within the RACH procedure [24]).

In this work, a dynamic mode selection scenario is considered, where all potential D2D users (i.e., the users in set $\mathbf{D}$) can be allocated either cellular or D2D mode based on results of resource allocation. Consequently, let us define the N-dimensional binary mode allocation vector $\mathbf{c} = [c_1(t), \ldots, c_N(t)]^T$ with the components $c_n(t)$, $n \in \mathbf{N}$, equaling 1 if U_n selects to operate in cellular mode at slot t, and 0 otherwise. Then, the set of all admissible values that the vector $\mathbf{c}$ can take is defined by

$$\mathbf{C} = \left\{ \mathbf{c} \,\middle|\, c_n(t) \in \{0,1\}, c_m(t) = 1, \forall n \in \mathbf{D}, \forall m \in \mathbf{C} \right\}. \quad (1)$$

An example of a network with $\mathbf{N} = \{1, \ldots, 12\}$ and $\mathbf{C} = \{4, 12\}$, the users U_3, U_4, U_6, U_9, U_{12} operating in cellular mode, and the rest of the users communicating in D2D mode, is shown in Figure 1.

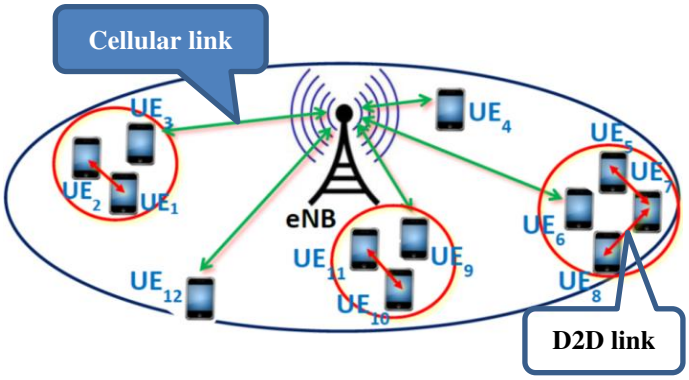

Fig. 1. Example of a network with $\mathbf{N} = \{1, \ldots, 12\}$, $\mathbf{C} = \{4, 12\}$, where UE_3, UE_4, UE_6, UE_9, UE_{12} operate in cellular mode.

B. Spectrum Usage

In LTE/LTE-A networks, the spectrum resources are allocated in terms of resource blocks (RBs). Each RB occupies 180 kHz in frequency domain, and has a slot-long duration in time domain. The RBs are assigned to cellular users by the eNB using a standard packet scheduling procedure [24]. The use of packet scheduling in a D2D-enabled LTE-A network is described in detail in [11].

In short, a packet scheduling process can be explained as follows. In the UL direction, each user is required to collect and transmit its buffer status information (i.e., the number of bits arrived to the buffer denoted $a_n(t)$, and the instantaneous buffer size in bits denoted $q_n(t)$) at every slot t. After collecting this data, each user transmits a scheduling request (SR) with its buffer status information to the eNB via a dedicated physical uplink control channel (PUCCH). After receiving all the SRs, the eNB allocates RBs to the users (according to a certain

[1] In this work, the term "proximity" means both the physical distance of the users to each other, and the channels conditions (such as pass loss).

scheduling algorithm), and responds to all the SRs by sending the scheduling grants (SGs) together with the allocation information to the corresponding users via physical downlink control channels (PDCCHs) [11]. In the DL, the eNB readily finds out the DL buffer status for each user, allocates RBs and sends the SGs together with the allocation information to the corresponding users via PDCCHs [11]. In the framework used in this paper, a described packet scheduling process is applied for cellular users. Resource allocation approach for D2D users is presented in Section V.

In our model, the total available bandwidth is assumed to be equal K RBs, numbered RB_1, ..., RB_K. Let $\mathbf{K} = \{1, \ldots, K\}$ be the set of RBs' indices comprising the bandwidth. Correspondingly, we define the $N \times K$-dimensional binary RB allocation matrix as

$$\mathbf{b} = \begin{bmatrix} b_1^1(t) & .. & b_1^K(t) \\ : & : & : \\ b_N^1(t) & .. & b_N^K(t) \end{bmatrix}$$

with the components $b^k_n(t)$, $n \in \mathbf{N}$, $k \in \mathbf{B}$, equaling 1 if U_n is allocated RB_k at slot t, and 0 otherwise. Note that each RB can be allocated to at most one CU. Hence,

$$\sum_{n \in \mathbf{N}} c_n(t) b_n^k(t) \le 1, \forall k \in \mathbf{K}. \tag{2a}$$

The number of D2D users operating on the same RB is unlimited. Additionally, to maximize the network utilization, we enforce each RB to be allocated to at least one user, i.e.

$$\sum_{n \in \mathbf{N}} b_n^k(t) \ge 1, \forall k \in \mathbf{K}. \tag{2b}$$

Accordingly, the set of all admissible values that the matrix $\mathbf{b}$ can take is defined as

$$\mathbf{B} = \left\{ \mathbf{b} \,\middle|\, b_n(t) \in \{0,1\}, \sum_{m \in \mathbf{N}} c_m(t) b_m^k(t) \le 1, \sum_{m \in \mathbf{N}} b_m^k(t) \ge 1, \forall n \in \mathbf{N}, \forall k \in \mathbf{K} \right\}. \tag{2c}$$

C. Channel Model

In LTE system, both single carrier frequency division multiple access (SC-FDMA) applied in the UL direction, and orthogonal frequency division multiple access (OFDMA) applied in the DL direction, provide orthogonality of RB allocation to different cellular users. This allows to attain a minimal level of co-channel interference for CUs located within one cell [23]. In a considered network, the UL and DL transmissions of CU may be distorted by DUs operating on the same RBs as this CU. On the other hand, the transmissions of DU may be distorted not only by the CUs, but also by other DUs operating on the same RBs as this DU.

Let G^k_{nm}, $n \in \mathbf{N}$, $m \in \mathbf{N}$, $k \in \mathbf{K}$ denote the channel gain coefficient between the transmitter-receiver pair of U_n and U_m operating on RB_k. Note, that in LTE the instantaneous values of G^k_{nm} for UL and DL directions can be obtained from the CSI through the use of the reference signals (RSs) [11]. Let us also define the N-dimensional non-negative power allocation vector $\mathbf{p} = [p_1(t), \ldots, p_N(t)]^T$ with the components $p_n(t)$, $n \in \mathbf{N}$, $m \in \mathbf{N}$ being the transmission power (in Watts) allocated to U_n at slot t.

Note, that if user U_n is allocated a cellular mode (i.e., $c_n(t) = 1$) then at any slot t, the SINR for U_n operating on RB_k equals

$$SINR_n^k(t) = \frac{p_n(t) b_n^k(t) G_{nn}^k}{\sum_{m \in \mathbf{N} \setminus \{n\}} (1 - c_m(t)) p_m(t) b_n^k(t) b_m^k(t) G_{mn}^k + N_n}, \forall n \in \mathbf{N}, \forall k \in \mathbf{K}. \tag{4a}$$

The denominator of (4a) is a sum of the following two components: the thermal noise power in the channel of U_n given by N_n, and the interference from the DUs operating on RB_k, given by

$$I_n^k(t) = c_n(t) \sum_{m \in \mathbf{N} \setminus \{n\}} (1 - c_m(t)) p_m(t) b_n^k(t) b_m^k(t) G_{mn}^k, \forall n \in \mathbf{N}, \forall k \in \mathbf{K}. \tag{4b}$$

On the other hand, if U_n is allocated a D2D mode ($c_n(t) = 0$), then the SINR at slot t for U_n operating on RB_k equals

$$SINR_n^k(t) = \frac{p_n(t) b_n^k(t) G_{nn}^k}{\sum_{m \in \mathbf{N} \setminus \{n\}} p_m(t) b_n^k(t) b_m^k(t) G_{mn}^k + N_n}, \forall n \in \mathbf{N}, \forall k \in \mathbf{K} \tag{5a}$$

with the interference from the CUs and DUs operating on RB_k, given by:

$$I_n^k(t) = (1 - c_n(t)) \sum_{m \in \mathbf{N} \setminus \{n\}} p_m(t) b_n^k(t) b_m^k(t) G_{mn}^k, \forall n \in \mathbf{N}, \forall k \in \mathbf{K}. \tag{5b}$$

Combining (4a) and (5a), we get the following general SINR expression for U_n operating on RB_k at any slot t in either mode:

$$SINR_n^k(t) = \frac{c_n(t) p_n(t) b_n^k(t) G_{nn}^k}{\sum_{m \in \mathbf{N} \setminus \{n\}} (1 - c_m(t)) p_m(t) b_n^k(t) b_m^k(t) G_{mn}^k + N_n} + \frac{(1 - c_n(t)) p_n(t) b_n^k(t) G_{nn}^k}{\sum_{m \in \mathbf{N} \setminus \{n\}} p_m(t) b_n^k(t) b_m^k(t) G_{mn}^k + N_n}, \forall n \in \mathbf{N}, \forall k \in \mathbf{K}. \tag{6}$$

In (4) and (5), the transmission power of the users cannot exceed some predefined limits. Let P_n and P_{eNB} be the maximal possible transmission power levels (in Watts) of U_n and the eNB, respectively. Then, for cellular users:

$$0 \le c_n(t) p_n(t) \le P_n, \forall n \in \mathbf{N} \tag{7a}$$

for the UL direction, and

$$0 \le \sum_{n \in \mathbf{N}} c_n(t) p_n(t) \le P_{eNB}. \tag{7b}$$

for the DL direction. For D2D users, we have

$$0 \le (1 - c_n(t)) p_n(t) \le P_n, \forall n \in \mathbf{N} \tag{7c}$$

in the UL and DL directions.

Accordingly, the set of all admissible values that the matrix $\mathbf{p}$ can take is defined as

$$\mathbf{P} := \left\{ \mathbf{p} \,\middle|\, 0 \le p_n(t) \le P_n, \forall n \in \mathbf{N} \right\} \tag{8a}$$

for the UL direction, and

$$\mathbf{P} = \left\{ \mathbf{p} \,\middle|\, 0 \le \sum_{n \in \mathbf{N}} c_n(t) p_n(t) \le P_{eNB}, 0 \le (1 - c_n(t)) p_n(t) \le P_n, \forall n \in \mathbf{N} \right\} \tag{8b}$$

for the DL direction.

III. Resource Allocation Problem

A. Problem Statement

The key advantage of D2D communication is the possibility of QoS provisioning within the cellular spectrum [27]. The key challenge here is the interference caused by DUs to CUs, and vice versa [27]. In many previous works (e.g., [7], [8]) the interference has been mitigated by introducing the algorithms of high computational complexity, and thus the application of

these methods to large-scale networks is unlikely. Hence, an efficient algorithm should (i) maximize QoS for both the DUs and CUs; (ii) guarantee interference protection of the users; (iii) have a low to moderate complexity.

To fulfil the first requirement of resource allocation, it is important to choose an appropriate and easily obtainable system parameter as a QoS measure. Traditionally, D2D communication has been viewed as a prominent tool for increasing the spectral efficiency of the network [27]. However, D2D communication can also be used to reduce delay and loss (which is very important for such real-time applications, as live streaming, video sharing, gaming, etc.). Unfortunately, in LTE system the direct estimation of delay and loss is rather complex. For instance, the packet end-to-end delay consists of various components, including transmission and queuing delays, propagation and processing delays, as well as delays due to scheduling and hybrid automatic repeat request (HARQ) [23]. The accurate analysis of these delay components requires knowledge of many system parameters which may be not available during resource allocation.

In this paper, the buffer size of UEs is used as a service performance measure, mainly because (i) it is directly related to the delay and loss, and (ii) at any slot t, it can be easily estimated using the well-known Lindley's equation [28]

$$q_n(t+1) = \lceil q_n(t) + a_n(t) - r_n(t) \rceil^+, \forall n \in \mathbf{N} \quad (9)$$

where $\lceil x \rceil^+ = \max(0, x)$; $r_n(t)$ is the number of bits served at the buffer of U_n at slot t. Note, that at any t the parameters $q_n(t)$ and $a_n(t)$ (representing buffer status information) are readily available at the corresponding U_n. The parameter $r_n(t)$ depends on the number of RBs and the transmission power allocated to U_n. In LTE/LTE-A, $r_n(t)$ can be found using the modified Shannon expression [29], given by

$$r_n(t) = \omega \cdot \psi \sum_{k \in \mathbf{K}} b_n^k(t) \log\left(1 + g(SINR_n^k(t)) \cdot SINR_n^k(t)\right), \forall n \in \mathbf{N}. \quad (10)$$

In (10), $SINR_n^k(t)$ is calculated using (6) for all $n \in \mathbf{N}$; ω is the bandwidth of one RB (ω = 180 kHz); ψ is the system bandwidth efficiency; a function $g(\cdot)$ determines the SINR efficiency of the transmission channel of U_n [33]. More detailed description of ψ and $g(\cdot)$ will be provided in the next subsection. An example of a described system model for the network depicted in Figure 1 is shown in Figure 2.

With buffer size as a QoS measure, at each slot t the resources can be allocated to minimize the maximal buffer size of the users at the next slot t+1. This will help to reduce the possibility of the network congestion, decrease delay and loss for the users.

To meet the second requirement of resource allocation, for each user in the network we specify some target interference level I_n^{tar}[2] and constrain the inference to each user to stay below I_n^{tar} for all $n \in \mathbf{N}$, i.e.:

$$\sum_{k \in \mathbf{K}} I_n^k(t) \le I_n^{tar}, \forall n \in \mathbf{N}.$$

Note that the values of I_n^{tar} can be set by the eNB (based on, e.g., QoS requirements of the users), and then sent to the corresponding users within a standard LTE SIP [25]. Alternatively, the users can specify their target interference levels themselves, and send this information to the eNB.

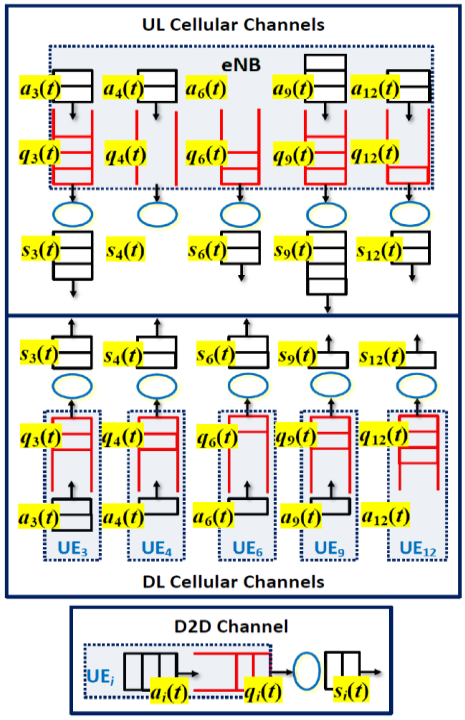

Fig. 2. A system model of the network illustrated in Figure 1 ($i \in \{1, 2, 5, 6, 7, 8, 9, 10, 11\}$ for D2D channels).

We are now ready to formulate the problem. For simplicity, the index t is skipped below and further in the paper. The considered problem is

$$\text{minimize} \quad \max_{n \in \mathbf{N}} \lceil q_n + a_n - r_n(\mathbf{b}, \mathbf{c}, \mathbf{p}) \rceil^+ \quad (11a)$$

$$\text{subject to:} \quad \mathbf{b} \in \mathbf{B}, \ \mathbf{c} \in \mathbf{C}, \ \mathbf{p} \in \mathbf{P} \quad (11b)$$

$$c_n \sum_{m \in \mathbf{N} \setminus \{n\}} (1 - c_m) p_m \sum_{k \in \mathbf{K}} b_n^k b_m^k G_{mn}^k \le I_n^{tar}, \forall n \in \mathbf{N} \quad (11c)$$

$$(1 - c_n) \sum_{m \in \mathbf{N} \setminus \{n\}} p_m \sum_{k \in \mathbf{K}} b_n^k b_m^k G_{mn}^k \le I_n^{tar}, \forall n \in \mathbf{N} \quad (11d)$$

where $r_n(\cdot)$ is expressed explicitly as a function of **b, c** and **p**; the feasibility sets **B**, **C** and **P** are defined in (2c), (1) and (8), respectively.

Note that in (11), the values of a_n and q_n are known to U_n (and the eNB in case if a standard LTE packet scheduling procedure [24] is applied); the values of G_{nm} are known to U_n, U_m and the eNB (from the CSI through the use of LTE RSs [11]); the values of I_n^{tar} are known by U_n and the eNB. The information on the sets **C** and **D** is acquired by the eNB during session setups (from the SIP [24]) or upon user arrival to the network (within a RACH procedure [24]). A solution methodology for (11) is presented in Section IV.

B. Bandwidth and SINR Efficiency

In a real LTE/LTE-A system, the bandwidth efficiency and the SINR efficiency are strictly less than 1 due to numerous reasons [29]. The system bandwidth efficiency ψ is reduced due to several overheads on link and system levels. Therefore, it is fully determined by the design and internal settings of LTE

[2] Possible I_n^{tar} settings will be discussed in Section V.

system, and do not depend on the PHY characteristics of wireless channels.

The system SINR efficiency is mainly limited by the maximum efficiency of the supported modulation and coding scheme (MCS) [29]. In LTE, the appropriate MCS is selected according to the adaptive modulation and coding (AMC) algorithm to maximize the service rate by adjusting the transmission parameters to the current channel conditions. AMC is one of the realizations of dynamic link adaptation. In AMC algorithm, MCS parameter is adapted based on channel quality indicator (CQI) at every CQI Feedback Cycle (CFC), which can last one or several time slots. The higher MCS values are assigned to the channels with good channel quality (to achieve higher transmission rates). The lower MCS values are assigned to the channels with poor channel quality to decrease the transmission rates and, consequently, ensure the transmission quality [30], [31].

The basic MCS selection scheme is described as follows. The LTE standard allows 15 MCS indices. Based on instantaneous channel conditions and power allocations, the SINR of the wireless channels vary. Depending on SINR, the corresponding MCS index is chosen as [31]

$$MCS = \begin{cases} MCS_1, & SINR < \gamma_1 \\ MCS_2, & \gamma_1 \le SINR < \gamma_2 \\ \vdots & \vdots \\ MCS_{15}, & \gamma_{14} \le SINR < \gamma_{15} \end{cases} \quad (12)$$

where the values $\gamma_1 < \gamma_2 < \ldots < \gamma_{15}$ are the SINR thresholds for selecting the MCS index. Table I shows the MCS indexes k, the corresponding values of SINR threshold γ_k and the SINR efficiencies $\zeta^D{}_k$ and $\zeta^C{}_k$ for DUs and CUs, respectively.

Hence, the function $g(\cdot)$ is calculated using

$$g^C(SINR) = \begin{cases} \zeta_1^C, & SINR < \gamma_1 \\ \zeta_2^C, & \gamma_1 \le SINR < \gamma_2 \\ \vdots & \vdots \\ \zeta_{15}^C, & \gamma_{14} \le SINR < \gamma_{15} \end{cases} \quad (13b)$$

$$g^D(SINR) = \begin{cases} \zeta_1^D, & SINR < \gamma_1 \\ \zeta_2^D, & \gamma_1 \le SINR < \gamma_2 \\ \vdots & \vdots \\ \zeta_{15}^D, & \gamma_{14} \le SINR < \gamma_{15} \end{cases} \quad (13c)$$

for CUs and DUs, respectively. A general expression for $g(\cdot)$ is given by

$$g(SINR_n^k) = y_n \cdot g^C(SINR_n^k) + (1 - y_n) \cdot g^D(SINR_n^k), \forall n \in \mathbf{N}, \forall k \in \mathbf{K}. \quad (14)$$

It should be mentioned that it is possible to combine the allocation of transmission power with MCS selection (for enhancing the algorithm performance). This, however, will increase the algorithm complexity (since more parameters should be considered in problem formulation). Hence, we assume that the power allocations are conducted independently of the MCS adaptation (i.e., the results of resource allocation will have no effect on selected MCS values).

TABLE I
CQI-MCS MAPPING FOR D2D AND CELLULAR LINKS [30], [31]

MCS index, k	Modulation	SINR Thresholds (dB), γ_k	SINR Efficiency for DUs, $\zeta^D{}_k$	Min. Rate for DUs (kbps)	SINR Efficiency for DUs, $\zeta^C{}_k$	Min. Rate for CUs (kbps)
0	No transmission					
1	QPSK	-3.1	0.1667	28.00	0.1523	25.59
2	QPSK	-1.2	0.2222	37.33	0.2344	39.38
3	QPSK	1.5	0.3333	56.00	0.3770	63.34
4	QPSK	4	0.6667	112.00	0.6016	101.07
5	QPSK	6	1.0000	168.00	0.8770	147.34
6	QPSK	8.9	1.2000	201.60	1.1758	197.53
7	16-QAM	12.7	1.3333	224.00	1.4766	248.07
8	16-QAM	14.9	2.0000	336.00	1.9141	321.57
9	16-QAM	17.5	2.4000	403.20	2.4063	404.26
10	64-QAM	20.5	3.0000	504.00	2.7305	458.72
11	64-QAM	22.5	3.0000	504.00	3.3223	558.72
12	64-QAM	23.2	3.6000	604.80	3.9023	655.59
13	64-QAM	24.9	4.5000	756.00	4.5234	759.93
14	64-QAM	27	5.0000	840.00	5.1152	859.35
15	64-QAM	29.1	5.5000	924.00	5.5547	933.19

IV. RESOURCE ALLOCATION ALGORITHM

Note, that the problem (11) is equivalent to

$$\text{minimize} \quad q_{\max} \quad (15a)$$

$$\text{subject to:} \quad \mathbf{b} \in \mathbf{B}, \mathbf{c} \in \mathbf{C}, \mathbf{p} \in \mathbf{P} \quad (15b)$$

$$c_n \sum_{m \in \mathbf{N} \setminus \{n\}} (1 - c_m) p_m \sum_{k \in \mathbf{K}} b_n^k b_m^k G_{mn}^k \le I_n^{tar}, \forall n \in \mathbf{N} \quad (15c)$$

$$(1 - c_n) \sum_{m \in \mathbf{N} \setminus \{n\}} p_m \sum_{k \in \mathbf{K}} b_n^k b_m^k G_{mn}^k \le I_n^{tar}, \forall n \in \mathbf{N} \quad (15d)$$

$$q_n + a_n - q_{\max} \le r_n(\mathbf{b}, \mathbf{c}, \mathbf{p}) \le q_n + a_n, \forall n \in \mathbf{N}. \quad (15e)$$

In above formulation, some of the optimization variables (particularly, the components of **b** and **c**) can take only binary values, whereas the other variables (the components of **p**) are real-valued. In addition, the constraints in (15e) depend on the non-smooth non-convex functions $r_n(\mathbf{b}, \mathbf{c}, \mathbf{p})$, $n \in \mathbf{N}$. Hence, (15) is a non-convex mixed integer non-linear programming problem (MINLP) problem, which is Nondeterministic Polynomial-time (NP) hard. For immediate proof of NP-hardness, note that MINLP includes mixed integer linear programming (MILP) problem, which is NP-hard [41].

A. Smooth Approximation

Before applying any MINLP method for solving (15), a non-smooth function $g(\cdot)$ in (14), included in the expression of $r_n(\mathbf{b}, \mathbf{c}, \mathbf{p})$ (given by (10)), should be replaced by its smooth approximation. To construct a smooth approximation of $g(x)$, note that this function is equivalent to the sum of the shifted and scaled versions of a well-known Heaviside step function $H(x)$ [38]. That is,

$$g(x)=\sum_{k=1}^{15}(\zeta_k-\zeta_{k-1})H(x-\gamma_k),\ H(x)=\begin{cases}1, & \text{if } x\ge 0\\ 0, & \text{otherwise}\end{cases} \quad (16)$$

where $\zeta_0 = 0$.

Recall, that a smooth approximation for a step function $H(x)$ is given by a logistic sigmoid function [39]:

$$\hat{H}_q(x)=\frac{1}{1+e^{-2qx}}$$

where $q > 0$, x is in range of real numbers from - ∞ to + ∞. If we take $H(0) = ½$, then a larger q corresponds to a closer transition to $H(x)$, i.e.

$$\lim_{q\to\infty}\hat{H}_q(x)=H(x).$$

Above holds, because for $x < 0$, we have

$$e^{-2qx}\to+\infty,\ \hat{H}_q(x)\approx H(x)=0;$$

for $x > 0$,

$$e^{-2qx}\to 0,\ \hat{H}_q(x)\approx H(x)=1;$$

for $x = 0$,

$$e^{-2qx}=1,\ \hat{H}_q(x)=H(x)=\frac{1}{2}.$$

Consequently, an approximation for a shifted Heaviside function is represented by a shifted logistic function

$$\hat{H}_q(x-\gamma_k)=\frac{1}{1+e^{-2q(x-\gamma_k)}} \quad (17)$$

defined for $q > 0$, with real x in range from - ∞ to + ∞. Based on (17), we can construct a smooth approximation for $g(x)$ as

$$\hat{g}_q(x)=\sum_{k=1}^{15}(\zeta_k-\zeta_{k-1})\hat{H}_q(x-\gamma_k)=\sum_{k=1}^{15}\frac{\zeta_k-\zeta_{k-1}}{1+e^{2q(x-\gamma_k)}}. \quad (18)$$

Then, it is rather straightforward to verify that

$$\lim_{q\to\infty}\hat{g}_q(x)=g(x).$$

With approximation given by (18), $r_n(\mathbf{b}, \mathbf{c}, \mathbf{p})$ appearing in the constraints (15e) will take the form

$$\hat{r}_n(\mathbf{b},\mathbf{c},\mathbf{p})=\omega\cdot\psi\sum_{k\in\mathbf{K}}b_n^k\log\left(1+\hat{g}(SINR_n^k)\cdot SINR_n^k\right),\ \forall n\in\mathbf{N}. \quad (19)$$

B. ADMM-Based Method for Solving Continuous Relaxation

Note, that in any MINLP method, the solution process involves solving a smooth continuous relaxation of the problem (the problem without integer restrictions). In our case, such relaxation is given by

$$\text{minimize}\ \ q_{\max} \quad (20a)$$

$$\text{subject to: } \mathbf{b}\in\tilde{\mathbf{B}},\mathbf{c}\in\tilde{\mathbf{C}},\mathbf{p}\in\mathbf{P} \quad (20b)$$

$$c_n\sum_{m\in\mathbf{N}\setminus\{n\}}(1-c_m)p_m\sum_{k\in\mathbf{K}}b_n^kb_m^kG_{mn}^k\le I_n^{tar},\forall n\in\mathbf{N} \quad (20c)$$

$$(1-c_n)\sum_{m\in\mathbf{N}\setminus\{n\}}p_m\sum_{k\in\mathbf{K}}b_n^kb_m^kG_{mn}^k\le I_n^{tar},\forall n\in\mathbf{N} \quad (20d)$$

$$q_n+a_n-q_{\max}\le\hat{r}_n(\mathbf{b},\mathbf{c},\mathbf{p})\le q_n+a_n,\forall n\in\mathbf{N} \quad (20e)$$

where

$$\tilde{\mathbf{C}}=\left\{\mathbf{c}\,\middle|\,0\le c_n\le 1,c_m=1,\forall n\in\mathbf{D},\forall m\in\mathbf{C}\right\}, \quad (20f)$$

$$\tilde{\mathbf{B}}=\left\{\mathbf{b}\,\middle|\,0\le b_n\le 1,\sum_{m\in\mathbf{N}}c_mb_m^k\le 1,\sum_{m\in\mathbf{N}}b_m^k\ge 1,\forall n\in\mathbf{N},\forall k\in\mathbf{K}\right\}. \quad (20g)$$

The above problem is cast as a non-convex non-linear programming (NLP) problem, which is NP-hard (see [32] for a proof). In general, the non-convex NLP problems can be solved using either exact (deterministic) or heuristic algorithms. Example of an exact method is a standard interior-point method [33] modified for non-convex problems (as it has been done, for instance, in [34]). Examples of heuristic techniques are the alternate minimization (e.g., [35]) and various search methods (such as genetic algorithm [36]).

Additionally, a number of parallelization techniques (e.g., particle swarm optimization [10] or evolutionary algorithms [37]) can be deployed to speed up a solution process of the exact methods. In these techniques, a large problem is divided into a number of smaller, easy to solve sub-problems [16]. One of the approaches to decompose the original problem has been proposed in ADMM [15]. ADMM provides a robust convex optimization approach with guaranteed global convergence at $O(1/\varepsilon)$ rate (where ε is an error) even when the functions are non-smooth [17]. At first, the modifications of ADMM have been successfully applied for solving linear programming (LP) relaxations of the large-scale MILP problems. Examples of such methods include AD3 [18] and Bethe-ADMM [19].

More recently, the variety of ADMM techniques have been used to solve the continuous relaxations of large-scale non-convex MINLP problems in application to optimal power flow in microgrids [20], discrete labeling in random fields [21], and gas transportation problems [22]. Although without guaranteed convergence to the global optimum, results reported in [20] – [22] have demonstrated that the memory and computation complexities of these techniques are only of the orders of the size of sub-problems. Hence, these techniques are applicable to our problem. In the following, it will be shown how a common approach presented in [20] – [22] can be used to solve (20).

Note that the formulation (20) (and also (15)) involves the so-called global optimization variables **b**, **c** and **p**. A common technique to decouple the problem (20) is to create N local "copies" $\mathbf{b}_{(1)}, \ldots, \mathbf{b}_{(N)}$, $\mathbf{c}_{(1)}, \ldots, \mathbf{c}_{(N)}$ and $\mathbf{p}_{(1)}, \ldots, \mathbf{p}_{(N)}$ of the global variables **b**, **c** and **p**, respectively, such that

$$\mathbf{b}_{(n)}=\begin{bmatrix}b_{1(n)}^1 & .. & b_{N(n)}^K\\ : & : & :\\ b_{N(n)}^1 & .. & b_{N(n)}^K\end{bmatrix},\ \mathbf{c}_{(n)}=\begin{bmatrix}c_{1(n)}\\ :\\ c_{N(n)}\end{bmatrix},\ \mathbf{p}_{(n)}=\begin{bmatrix}p_{1(n)}\\ :\\ p_{N(n)}\end{bmatrix},\forall n\in\mathbf{N}. \quad (21)$$

After this, all N local variables are constrained to be equal, and the following (equivalent to (20)) problem is defined:

$$\text{minimize}\ \ q_{\max} \quad (22a)$$

$$\text{subject to: } \mathbf{b}_{(n)}\in\tilde{\mathbf{B}},\ \mathbf{c}_{(n)}\in\tilde{\mathbf{C}},\ \mathbf{p}_{(n)}\in\mathbf{P} \quad (22b)$$

$$c_{n(n)}\sum_{m\in\mathbf{N}\setminus\{n\}}(1-c_{m(n)})p_{m(n)}\sum_{k\in\mathbf{K}}b_{n(n)}^kb_{m(n)}^kG_{mn}^k\le I_n^{tar},\forall n\in\mathbf{N} \quad (22c)$$

$$(1-c_{n(n)})\sum_{m\in\mathbf{N}\setminus\{n\}}p_{m(n)}\sum_{k\in\mathbf{K}}b_{n(n)}^kb_{m(n)}^kG_{mn}^k\le I_n^{tar},\forall n\in\mathbf{N} \quad (22d)$$

$$q_n+a_n-q_{\max}\le\hat{r}_n(\mathbf{b}_{(n)},\mathbf{c}_{(n)},\mathbf{p}_{(n)})\le q_n+a_n,\forall n\in\mathbf{N} \quad (22e)$$

$$\mathbf{b}_{(1)}=\ldots=\mathbf{b}_{(N)},\ \mathbf{c}_{(1)}=\ldots=\mathbf{c}_{(N)},\ \mathbf{p}_{(1)}=\ldots=\mathbf{p}_{(N)}. \quad (22f)$$

The problem (22) can be transformed to the canonical form as follows

$$\text{minimize}\ \ q_{\max}+\sum_{n\in\mathbf{N}}I_{\mathbf{F}_{(n)}}(\mathbf{b}_{(n)},\mathbf{c}_{(n)},\mathbf{p}_{(n)}) \quad (23a)$$

$$\text{subject to: } \mathbf{b}_{(1)} = ... = \mathbf{b}_{(N)},\ \mathbf{c}_{(1)} = ... = \mathbf{c}_{(N)},\ \mathbf{p}_{(1)} = ... = \mathbf{p}_{(N)}. \quad (23b)$$

In (23), $\mathbf{F}_{(n)}$, $n \in \mathbf{N}$, are the feasibility sets defined by

$$\mathbf{F}_{(n)} = \left\{ \mathbf{b}_{(n)}, \mathbf{c}_{(n)}, \mathbf{p}_{(n)} \;\middle|\; \begin{array}{c} \mathbf{b}_{(n)} \in \tilde{\mathbf{B}},\ \mathbf{c}_{(n)} \in \tilde{\mathbf{C}},\ \mathbf{p}_{(n)} \in \mathbf{P} \\ c_{n(n)} \sum\limits_{m \in \mathbf{N} \setminus \{n\}} (1 - c_{m(n)}) p_{m(n)} \sum\limits_{k \in \mathbf{K}} b^k_{n(n)} b^k_{m(n)} G^k_{mn} \le I^{tar}_n \\ (1 - c_{n(n)}) \sum\limits_{m \in \mathbf{N} \setminus \{n\}} p_{m(n)} \sum\limits_{k \in \mathbf{K}} b^k_{n(n)} b^k_{m(n)} G^k_{mn} \le I^{tar}_n \\ q_n + a_n - q_{\max} \le \hat{r}_n(\mathbf{b}_{(n)}, \mathbf{c}_{(n)}, \mathbf{p}_{(n)}) \le q_n + a_n \end{array} \right\}; \quad (24a)$$

$I_{\mathbf{F}(n)}(\cdot)$, $n \in \mathbf{N}$, are the indicator functions of $\mathbf{F}_{(n)}$, given by

$$I_{F_{(n)}}(\mathbf{b}_{(n)}, \mathbf{c}_{(n)}, \mathbf{p}_{(n)}) = \begin{cases} 0, & \mathbf{b}_{(n)}, \mathbf{c}_{(n)}, \mathbf{p}_{(n)} \in \mathbf{F}_{(n)} \\ +\infty, & \mathbf{b}_{(n)}, \mathbf{c}_{(n)}, \mathbf{p}_{(n)} \notin \mathbf{F}_{(n)} \end{cases}. \quad (24b)$$

After this, ADMM can be applied to solve (23). A detailed description of ADMM, also known as Douglas-Rachford splitting, can be found in [15]. In short, ADMM can be applied to the problems of a kind

$$\text{minimize} \quad \sum_{n \in \mathbf{N}} f_n(x_n) + g(z) \quad (25a)$$

$$\text{subject to: } x_n = z, \forall n \in \mathbf{N}. \quad (25b)$$

To solve the above problem, ADMM uses the method of multipliers concatenated with an iteration of the Gauss-Seidel algorithm [40], i.e., it iterates on i as shown below [15]:

$$x_n^{i+1} = \arg\min_{x_n} \left\{ f_n(x_n) + \frac{1}{2\lambda} \left\| x_n - z^i + u_n^i \right\|_2^2 \right\}, \quad (26a)$$

$$z^{i+1} = \frac{1}{N} \sum_{n \in \mathbf{N}} (x_n^{i+1} + u_n^i), \quad (26b)$$

$$u_n^{i+1} = u_n^i + x_n^{i+1} - z^{i+1}. \quad (26c)$$

Here x^i_n and z^i are the i^{th} updates of the optimization variables x_n and z, respectively; u^i_n is the i^{th} update of a scaled dual variable u_n; $\|\cdot\|_2$ is the Euclidean norm; $0 < \lambda \le 1/L$, where L is the Lipschitz constant [39] of $\nabla f_n(x_n)$.

The algorithm (26) can be further simplified as follows. Taking the average (over n) of (26b) and (26c), we obtain the following system of equations:

$$z^{i+1} = \bar{x}_n^{i+1} + \bar{u}_n^i, \quad (27a)$$

$$\bar{u}_n^{i+1} = \bar{u}^i + \bar{x}_n^{i+1} - \bar{z}_n^{i+1}. \quad (27b)$$

Solving (27) gives us $\bar{u}_n^{i+1} = 0$, and therefore z^{i+1} reduces to $\bar{x}^{i+1}$ (see (26b)). With these simplifications, we arrive at the following algorithm:

$$x_n^{i+1} = \arg\min_{x_n} \left\{ f_n(x_n) + \frac{1}{2\lambda} \left\| x_n - \bar{x}^i + u_n^i \right\|_2^2 \right\}, \quad (28a)$$

$$u_n^{i+1} = u_n^i + x_n^{i+1} - \bar{x}^{i+1}. \quad (28b)$$

Now, (28) can be applied to solve (23) as follows:

$$\mathbf{b}_{(n)}^{i+1} = \arg\min_{\mathbf{b}_{(n)}} \left\{ q_{\max} + I_{\mathbf{F}_{(n)}}(\mathbf{b}_{(n)}, \mathbf{c}_{(n)}, \mathbf{p}_{(n)}) + \frac{\left\| \mathbf{b}_{(n)} - \bar{\mathbf{b}}^i + \mathbf{u}_{(n)}^i \right\|_2^2}{2\lambda} \right\}, \quad (29a)$$

$$\mathbf{c}_{(n)}^{i+1} = \arg\min_{\mathbf{c}_{(n)}} \left\{ q_{\max} + I_{\mathbf{F}_{(n)}}(\mathbf{b}_{(n)}, \mathbf{c}_{(n)}, \mathbf{p}_{(n)}) + \frac{\left\| \mathbf{c}_{(n)} - \bar{\mathbf{c}}^i + \mathbf{v}_{(n)}^i \right\|_2^2}{2\lambda} \right\}, \quad (29b)$$

$$\mathbf{p}_{(n)}^{i+1} = \arg\min_{\mathbf{p}_{(n)}} \left\{ q_{\max} + I_{\mathbf{F}_{(n)}}(\mathbf{b}_{(n)}, \mathbf{c}_{(n)}, \mathbf{p}_{(n)}) + \frac{\left\| \mathbf{p}_{(n)} - \bar{\mathbf{p}}^i + \mathbf{w}_{(n)}^i \right\|_2^2}{2\lambda} \right\}, \quad (29c)$$

$$\mathbf{u}_{(n)}^{i+1} := \mathbf{u}_{(n)}^i + \mathbf{b}_{(n)}^{i+1} - \bar{\mathbf{p}}^{i+1}, \quad (29d)$$

$$\mathbf{v}_{(n)}^{i+1} := \mathbf{v}_{(n)}^i + \mathbf{c}_{(n)}^{i+1} - \bar{\mathbf{b}}^{i+1}, \quad (29e)$$

$$\mathbf{w}_{(n)}^{i+1} := \mathbf{w}_{(n)}^i + \mathbf{p}_{(n)}^{i+1} - \bar{\mathbf{y}}^{i+1}. \quad (29f)$$

In (29), $\mathbf{b}^i_{(n)}$ and $\mathbf{u}^i_{(n)}$ are the i^{th} updates of the optimization variable $\mathbf{b}_{(n)}$ and its scaled dual variable $\mathbf{u}_{(n)}$, respectively; $\mathbf{c}^i_{(n)}$ and $\mathbf{v}^i_{(n)}$ are the i^{th} updates of the optimization variable $\mathbf{c}_{(n)}$ and its scaled dual variable $\mathbf{v}_{(n)}$, respectively; $\mathbf{p}^i_{(n)}$ and $\mathbf{w}^i_{(n)}$ are the i^{th} updates of the optimization variable $\mathbf{p}_{(n)}$ and its scaled dual variable $\mathbf{w}_{(n)}$, respectively; $\bar{\mathbf{b}}^i$, $\bar{\mathbf{c}}^i$, $\bar{\mathbf{p}}^i$ are the i^{th} update averages of $\mathbf{b}^i_{(n)}$, $\mathbf{c}^i_{(n)}$ and $\mathbf{p}^i_{(n)}$, respectively. The search starts with $\mathbf{u}^0_{(n)} = 0$, $\mathbf{v}^0_{(n)} = 0$, $\mathbf{w}^0_{(n)} = 0$[3], and stops when $\mathbf{b}^i_{(n)} = \mathbf{b}^{i-1}_{(n)}$, $\mathbf{c}^i_{(n)} = \mathbf{c}^{i-1}_{(n)}$ and $\mathbf{p}^i_{(n)} = \mathbf{p}^{i-1}_{(n)}$.

As follows from (29), a proposed iterative resource allocation algorithm consists of two steps. At step 1 (equations (29a) – (29c)), the searches of primal and dual updates are conducted in parallel by N local computing processors. At step 2 (equations (29d) - (29f)), all the local variables $\mathbf{b}^i_{(n)}$, $\mathbf{c}^i_{(n)}$ and $\mathbf{p}^i_{(n)}$ are averaged (using, e.g., broadcasting) and the result is given to each local processor. The implementation of the algorithm (29) in the considered network model is described in Section V. Note, that the number of variables in problems (29a) – (29c) is N times less than that in the original problem (20). Consequently, by applying the algorithm in (29), the complexity of solving (20) can be significantly reduced. In this paper, a second-order interior point algorithm modified for non-convex problems (described in detail in [34]) is used to solve (29a) - (29c). This method has been chosen mainly due to its (relatively) low complexity - the worst-case complexity of a second-order interior point algorithm for smooth constrained nonconvex problems is $O(\varepsilon^{-3/2})$ (see [40] for a proof).

C. Feasibility Pump Heuristic for Solving MINLP

After the problem (29) is solved, we should apply some suitable technique to find optimal/near-optimal result. A typical deterministic method for solving MINLPs is a well-known branch-and-bound algorithm and its various modifications [42]. Some examples of heuristic approaches are [43] - [45]. In this paper, a Feasibility Pump (FP) heuristic for non-convex MINLPs ([45], [46]) is applied to solve (34). FP algorithm is perhaps the most simple and most effective for producing more and better solutions in a shorter average running time. For the problems with non-binary integer variables, the FP's complexity is exponential in size of a problem. For the problems with binary variables, its complexity is polynomial [47]. The local convergence properties of FP algorithm for non-convex problems have been proved in [46].

A fundamental idea of FP heuristic is to decompose the problem into two parts: integer feasibility and constraint feasibility. The former is achieved by rounding (solving a convex relaxation to the original problem), the latter - by projection (solving a continuous relaxation). Consequently, two

[3] Initial settings of $\mathbf{b}^0_n$, $\mathbf{c}^0_n$ and $\mathbf{p}^0_n$ will be discussed in Section 6.

sequences of points are generated. The first sequence, $\left\{(\overline{\mathbf{b},\mathbf{c},\mathbf{p}})_j\right\}_{j=1}^{J}$, $J = 1, 2, \ldots$, contains the integral points that may violate the non-convex constraints. The second sequence, $\left\{(\underline{\mathbf{b},\mathbf{c},\mathbf{p}})_j\right\}_{j=1}^{J}$, contains the points which are feasible for a continuous relaxation to the original problem but might not be integral. More specifically, with input $(\underline{\mathbf{b},\mathbf{c},\mathbf{p}})_1$ being a solution to (29), the algorithm generates two sequences by solving the following problems for $j = 1, \ldots, J$:

$$(\overline{\mathbf{b},\mathbf{c},\mathbf{p}})_j = \arg\min \left\|(\mathbf{b},\mathbf{c},\mathbf{p}) - (\underline{\mathbf{b},\mathbf{c},\mathbf{p}})_j\right\|_1 \tag{30a}$$

$$\text{subject to: } \mathbf{b}\in\mathbf{B}, \mathbf{c}\in\mathbf{C}, \mathbf{p}\in\mathbf{P} \tag{30b}$$

$$c_n \sum_{m\in\mathbf{N}\setminus\{n\}} (1-c_m) p_m \sum_{k\in\mathbf{K}} b_n^k b_m^k G_{mn}^k \le I_n^{tar}, \forall n\in\mathbf{N} \tag{30c}$$

$$(1-c_n) \sum_{m\in\mathbf{N}\setminus\{n\}} p_m \sum_{k\in\mathbf{K}} b_n^k b_m^k G_{mn}^k \le I_n^{tar}, \forall n\in\mathbf{N}; \tag{30d}$$

$$(\underline{\mathbf{b},\mathbf{c},\mathbf{p}})_{j+1} = \arg\min \left\|(\mathbf{b},\mathbf{c},\mathbf{p}) - (\overline{\mathbf{b},\mathbf{c},\mathbf{p}})_j\right\|_2 \tag{31a}$$

$$\text{subject to: } \mathbf{b}\in\widetilde{\mathbf{B}}, \mathbf{c}\in\widetilde{\mathbf{C}}, \mathbf{p}\in\mathbf{P} \tag{31b}$$

$$c_n \sum_{m\in\mathbf{N}\setminus\{n\}} (1-c_m) p_m \sum_{k\in\mathbf{K}} b_n^k b_m^k G_{mn}^k \le I_n^{tar}, \forall n\in\mathbf{N} \tag{31c}$$

$$(1-c_n) \sum_{m\in\mathbf{N}\setminus\{n\}} p_m \sum_{k\in\mathbf{K}} b_n^k b_m^k G_{mn}^k \le I_n^{tar}, \forall n\in\mathbf{N} \tag{31d}$$

$$q_n + a_n - q_{\max} \le \hat{r}_n(\mathbf{b},\mathbf{c},\mathbf{p}) \le q_n + a_n, \forall n\in\mathbf{N} \tag{31e}$$

where $\|\cdot\|_1$ and $\|\cdot\|_2$ are l_1 norm and l_2 norm, respectively. The rounding step is carried out by solving the problem (30), whereas the projection is the solution to (31). A suggested FP algorithm alternates between the rounding and projection steps until $(\overline{\mathbf{b},\mathbf{c},\mathbf{p}})_j = (\underline{\mathbf{b},\mathbf{c},\mathbf{p}})_j$ (which implies feasibility) or the number of iterations j has reached the predefined limit J. The workflow of a corresponding FP algorithm is presented in Figure 3.

Note that (31) is very similar to (20), and therefore it can be solved using the same ADMM-based technique. Problem (30) is the convex MINLP which can be solved to optimality by at least five different algorithms: branch-and-bound, generalized Benders decomposition, outer approximation, branch-and-cut algorithm and the extended cutting plane technique [48]. In this work, the modification of a branch-and-bound technique proposed in [42] has been used to solve (30).

0. **Initialization:** input J; set $j := 1$; solve (20) to obtain $(\underline{\mathbf{b},\mathbf{c},\mathbf{p}})_j$;
1. **If** $(\underline{\mathbf{b},\mathbf{c},\mathbf{p}})_j$ is feasible **then** goto step 7;
2. **While** ($j < J$) do: **{**
3. **Rounding:** solve (30) to obtain $(\overline{\mathbf{b},\mathbf{c},\mathbf{p}})_j$;
4. **If** ($(\overline{\mathbf{b},\mathbf{c},\mathbf{p}})_j = (\underline{\mathbf{b},\mathbf{c},\mathbf{p}})_j$) **then** goto step 7;
5. **Projection:** solve (31) to obtain $(\underline{\mathbf{b},\mathbf{c},\mathbf{p}})_{j+1}$;
6. Set $j := j + 1$; **}**
7. **Output:** solution $(\mathbf{b},\mathbf{c},\mathbf{p})^* := (\underline{\mathbf{b},\mathbf{c},\mathbf{p}})_j$.

Fig. 3. FP algorithm for solving a non-convex MINLP.

V. Algorithm Implementation

A. Implementation in LTE-D System

Note that the problem (11) describes a general resource allocation procedure where DUs and CUs can access both the UL and the DL spectrum resources of the eNB. However, according to the current 3rd Generation Partnership Project (3GPP) Release 12 specifications, CUs can occupy only the DL spectrum resources, whereas the UL resources are reserved for D2D communications ([31], [49]). Hence, in order to apply a proposed resource allocation method to a standard LTE-Direct (LTE-D) network, we have to make some modifications to formulation (11). In the following, we present two versions of the algorithm for resource allocation in LTE-D system. Discussion through the rest of the paper is applicable to both Frequency Division Duplex (FDD) and Time Division Duplex (TDD) LTE operation modes.

1) The Algorithm with the Controlled Power Levels of UEs

Since different channels (UL and DL) are reserved for CUs and DUs, there is no interference between cellular and D2D users, i.e. $c_n(1\text{-}c_m)b^k{}_n b^k{}_m = 0$, for all $n\in\mathbf{N}$, $m\in\mathbf{N}$, $k\in\mathbf{K}$. The interference exists only between the DUs operating on the same RBs and hence, the SINRs expression in (6) will transform to

$$SINR_n^k = \frac{c_n p_n b_n^k G_{nn}^k}{N_n} + \frac{(1-c_n) p_n b_n^k G_{nn}^k}{\sum_{m\in\mathbf{N}\setminus\{n\}} (1-c_m) p_m b_n^k b_m^k G_{mn}^k + N_n}, \forall n\in\mathbf{N}, \forall k\in\mathbf{K} \tag{32a}$$

where the interference for U_n (caused by other DUs operating on RB_k) is given by

$$I_n^k = (1-c_n) \sum_{m\in\mathbf{N}\setminus\{n\}} (1-c_m) p_m b_n^k b_m^k G_{mn}^k, \forall n\in\mathbf{N}, \forall k\in\mathbf{K}. \tag{32b}$$

Consequently, a feasibility set for matrix $\mathbf{b}$ transforms to

$$\mathbf{B} = \left\{ \mathbf{b} \;\middle|\; \begin{array}{c} b_n\in\{0,1\}, \sum_{m\in\mathbf{N}} c_m b_m^k \le 1, \sum_{m\in\mathbf{N}} b_m^k \ge 1, \sum_{m\in\mathbf{N}} c_m (1-c_j) b_m^k b_j^k = 0 \\ \forall n\in\mathbf{N}, \forall j\in\mathbf{N}, \forall k\in\mathbf{K} \end{array} \right\}. \tag{33}$$

Then, a resource allocation problem takes form

$$\text{minimize } \max_{n\in\mathbf{N}} \left\lceil q_n + a_n - r_n(\mathbf{b},\mathbf{c},\mathbf{p}) \right\rceil^+ \tag{34a}$$

$$\text{subject to: } \mathbf{b}\in\mathbf{B},\ \mathbf{c}\in\mathbf{C},\ \mathbf{p}\in\mathbf{P} \tag{34b}$$

$$(1-c_n) \sum_{m\in\mathbf{N}\setminus\{n\}} (1-c_m) p_m \sum_{k\in\mathbf{K}} b_n^k b_m^k G_{mn}^k \le I_n^{tar}, \forall n\in\mathbf{N}. \tag{34c}$$

Similar to (11), above problem is a non-smooth non-convex MINLP, and therefore it can be solved using the same solution method. Note however, that the complexity of (34) is lower than the complexity of (11), since the number of constraints in (34) is less than that in (11).

2) The Algorithm with Fixed Power Levels of UEs

In this paper, we also propose a simplified version of the algorithm for LTE-D system. In this modification, each user U_n, $n\in\mathbf{N}$, can be either in active state, where it transmits data with some fixed transmission power level equal P_n, or in idle state with transmission power level P_0 close to 0. In this case, a resource allocation problem is given by

$$\text{minimize } \max_{n\in\mathbf{N}} \left\lceil q_n + a_n - r_n(\mathbf{b},\mathbf{c}) \right\rceil^+ \tag{35a}$$

$$\text{subject to: } \mathbf{b} \in \mathbf{B},\ \mathbf{c} \in \mathbf{C} \tag{35b}$$

$$(1-c_n)\sum_{m\in\mathbf{N}\setminus\{n\}}(1-c_m)P_m\sum_{k\in\mathbf{K}}b_n^k b_m^k G_{mn}^k \le I_n^{tar}, \forall n\in\mathbf{N} \tag{35c}$$

with

$$SINR_n^k = \frac{c_n P_n b_n^k G_{nn}^k}{N_n} + \frac{(1-c_n)P_n b_n^k G_{nn}^k}{\sum_{m\in\mathbf{N}\setminus\{n\}}(1-c_m)P_m b_n^k b_m^k G_{mn}^k + N_n}, \forall n\in\mathbf{N}, \forall k\in\mathbf{K}. \tag{35d}$$

The above problem is a non-smooth non-convex integer programming problem (since all the variables are binary), which can be solved using a technique presented in Section IV. Note that the complexity of (35) is lower than the complexity of (34), because the number of variables is reduced from $N\times(K+2)$ to $N\times(K+1)$.

B. Target Interference Levels

In our network, some of the users may operate on very noisy channels, and further reduction of SINR in these channels will be disastrous. To indicate such channels, for each user on each RB, we set a certain target SINR level, denoted $SINR^{tar}$, below which the data transmission is considered unsatisfactory. Then, at any slot t, the SINR should be kept at the level

$$SINR_n^k = \frac{p_n b_n^k G_{nn}^k}{\sum_{m\in\mathbf{N}\setminus\{n\}}(1-c_m)p_m b_n^k b_m^k G_{mn}^k + N_n} \ge SINR^{tar}, \forall n\in\mathbf{N}, \forall k\in\mathbf{K} \tag{36a}$$

for users operating in cellular mode, and

$$SINR_n^k = \frac{p_n b_n^k G_{nn}^k}{\sum_{m\in\mathbf{N}\setminus\{n\}} p_m b_n^k b_m^k G_{mn}^k + N_n} \ge SINR^{tar}, \forall n\in\mathbf{N}, \forall k\in\mathbf{K}. \tag{36b}$$

for user operating in D2D mode.

Consequently, the interfering CUs and DUs are allowed to transmit at the levels

$$\sum_{k\in\mathbf{K}} I_n^k \le \frac{c_n p_n \sum_{k\in\mathbf{K}} b_n^k G_{nn}^k}{SINR^{tar}} - N_n = I_n^{tar}, \forall n\in\mathbf{N}, \tag{37a}$$

$$\sum_{k\in\mathbf{K}} I_n^k \le \frac{(1-c_n) p_n \sum_{k\in\mathbf{K}} b_n^k G_{nn}^k}{SINR^{tar}} - N_n = I_n^{tar}, \forall n\in\mathbf{N}. \tag{37b}$$

Combining (37a) and (37b), we arrive at

$$I_n^{tar} = \frac{1}{2}\left(\frac{p_n \sum_{k\in\mathbf{K}} b_n^k G_{nn}^k}{SINR^{tar}} - N_n\right), \forall n\in\mathbf{N}. \tag{38}$$

Note that right-hand side of (38) depends on the values of $\mathbf{p}$ which are unknown at the beginning of slot t (i.e. before resource allocation). Therefore, we deploy past (available) observations of $\mathbf{p}$, and set

$$I_n^{tar} = \frac{1}{2}\left(\frac{\bar{p}_n \sum_{k\in\mathbf{K}} b_n^k G_{nn}^k}{SINR^{tar}} - N_n\right), \quad \bar{p}_n = \frac{\sum_{\tau=1}^{T} p(t-\tau)}{T}, \ \forall n\in\mathbf{N}. \tag{39}$$

where T is the number of past observations; $\bar{p}_n$, $n \in \mathbf{N}$, is the average value of p_n during the period $[t-1, t-T]$. Note, that for algorithm implementations in LTE-D system (described in previous subsection), the target interference levels can be set using similar considerations.

C. Resource Allocation Procedure

In this paper, two different implementation schemes of the algorithm presented in Sections III and IV are considered. The first scheme, called Real-Time (RT), utilizes a centralized resource allocation (as described in [11]). In this scheme, RB, mode and power assignments are carried by the eNB for both the CUs and DUs. The corresponding procedure (repeated at the beginning of each slot t) is described as follows.

In the UL direction, all of the users (DUs and CUs) collect their instantaneous buffer status information and send it to the eNB using SRs via dedicated PUCCHs. After receiving all the SRs, the eNB solves (11) using FP algorithm shown in Figure 1. After getting an optimal solution $(\mathbf{b}, \mathbf{c}, \mathbf{p})^*$, the eNB transmits the SGs containing the RB, mode and power allocations to the corresponding users via PDCCHs. In the DL direction, the eNB determines the DL buffer status for all of the users operating in cellular mode, solves (11), and sends the SGs together with optimal allocations $(\mathbf{b}, \mathbf{c}, \mathbf{p})^*$ to the corresponding users via PDCCHs [11].

Note that at any slot t, RT scheme needs exactly two control signalling steps: step 1 with SRs transmitted by the users to the eNB; step 2 with the UL and DL optimal allocations sent by the eNB to the users. The main disadvantage of this scheme is related to delay due to UL scheduling, which may grow significantly when the number of users (equalling N in our case) sending the SRs at slot t is more than the number of LTE PUCCHs (see, e.g., [23], [50]).

In the second scheme, called Non-Real-Time (NRT), the growth of scheduling delay is avoided by increasing the duration of a resource allocation period (from one to $T > 1$ slots), and decreasing the number of SRs sent simultaneously within one slot. In this implementation, upon arrival of U_n, $n \in \mathbf{N}$ to the network, the random number τ_n from the interval $[0, T-1]$ is generated and stored in the memory of its device. The NRT scheme is repeated within each resource allocation period $[t, t+T-1]$, as follows.

In the UL direction, each user device updates its instantaneous buffers status information, calculates the average buffer status during the period $[t+\tau_n-T+1, t+\tau_n]$, given by

$$\bar{a}_n + \bar{q}_n = \frac{\sum_{i=0}^{T-1}\left(a(t+\tau_n-i)+q(t+\tau_n-i)\right)}{T}, \ \forall n\in\mathbf{N} \tag{40}$$

and transmits this information to the eNB via PUCCH at the beginning of slot τ_n.

After receiving the buffer status reports from all of the users (at slot $t+T-1$), the eNB replaces the instantaneous buffers status reports $a_n(t) + q_n(t)$ in (11) by the corresponding average values $\bar{a}_n + \bar{q}_n$, for all $n \in \mathbf{N}$. After getting an optimal solution $(\mathbf{b}, \mathbf{c}, \mathbf{p})^*$, the eNB sends the SGs containing the RB, mode and power allocations to corresponding users via PDCCHs. Note, that the determined optimal allocations will be valid for the next allocation period $[t+T, t+2T-1]$.

In the DL direction, the eNB collects the instantaneous DL buffer status and calculates the average buffer status for all of the users operating in cellular mode according to (40) for $\tau_n = t$

$+ T - 1$. After replacing the instantaneous buffers status reports $a_n(t) + q_n(t)$ in (11) by the corresponding average values $\bar{a}_n + \bar{q}_n$, the eNB finds a solution $(\mathbf{b}, \mathbf{c}, \mathbf{p})^*$, and transmits the SGs with the optimal allocations (for the next allocation period $[t + T, t + 2T - 1]$) to corresponding users via PDCCHs.

The main advantage of the above resource allocation procedure is reduced control signalling (the number of signalling steps in the second scheme is T times less than that in the first scheme). Additionally, the number of users simultaneously sending SRs in the second scheme is in general less than that in the first scheme, which helps to decrease the UL scheduling delay. The main drawback of the second resource allocation procedure is related to "non-real-time" allocation (since network resources are assigned based on the averaged, rather than instantaneous, buffer status values for a prolonged period T). This could potentially reduce the efficiency of a proposed NRT algorithm.

VI. Performance Evaluation

A. Simulation Settings

A simulation model of the network has been implemented upon a standard LTE-A platform using the OPNET simulation and development package [51]. The model consists of one eNBs and N users randomly positioned inside a three-sector hexagonal cell with antenna pattern specified in [30]. It is assumed that the users operate outdoors in a typical urban environment. Main simulation parameters of the model are listed in Table II.

TABLE II
Simulation Parameters of the Model

Parameter	Value
Cell radius	500 m
Frame Structure	Type 2 (TDD)
Slot duration	1 ms
TDD configuration	0
eNodeB max Tx power	46 dBm
UE max node Tx power	23 dBm
Noise power	-174 dBm/Hz
Path loss, cellular link	128.1 + 37.6 log(d), d[km]
NLOS path loss, D2D link	40 log(d) + 30 log(f) + 49, d[km], f[Hz]
LOS path loss, D2D link	16.9 log(d) + 20 log (f/5) + 46.8, d[m], f[GHz]
Shadowing st. dev.	10 dB (cell mode); 12 dB (D2D mode)

Discussion in this section mainly concerns the following schemes:

1) A general resource allocation procedure (formulated in (11)) with RT and NRT implementations. Further in the paper these schemes are referred to as G-RT (General RT algorithm) and G-NRT (General NRT algorithm), respectively.
2) The first version of the algorithm for LTE-D system with the controlled UEs' power levels (formulated in (34)) using RT and NRT implementations, referred to as 1-RT (1st algorithm with RT allocation) and 1-NRT (1st algorithm with NRT allocation), respectively.
3) The second version of the algorithm for LTE-D system with fixed UEs' power levels (formulated in (34)) using RT and NRT implementations, referred to as 2-RT (2nd algorithm with RT allocation) and 2-NRT (2nd algorithm with NRT allocation), respectively.

In all NRT schemes, the duration of a resource allocation period is set to be equal $T = 10$ slots. The allowed number of iterations in FP algorithm (see Figure 3) is limited to $J = 200$.

In the following, performance of the proposed resource allocation schemes is benchmarked with the performance of the following previously proposed algorithms: Energy-efficient Resource Sharing for mobile device-to-device multimedia communications (denoted ERS) described in [52], and Distributed Resource Allocation in D2D-enabled multi-tier cellular networks (denoted DRA) described in [5]. Unfortunately, there have been no prior works where the same objective (to minimize maximum buffer size of the users) has been considered. Hence, the relevance of the reference schemes has been determined mainly based on their ability to jointly perform mode selection, interference mitigation, spectrum management and power control. Both ERS and DRA partly satisfy this criterion. Particularly, ERS performs (for potential D2D pairs) a joint mode selection, power control and interference management with the objective to minimize the total transmission power of DUs. DRA allocates the spectrum and transmission power with the objective to maximize the sum rate of DUs and CUs, subject to interference constraints.

All of the schemes (G-RT/NRT, 1-RT/NRT, 2-RT/NRT, ERS, DRA) have been simulated with the settings listed in Table II. The user traffic in simulations has been modelled according to [53] using the Hypertext Transfer Protocol (HTTP) 1.1 model. According to the model, the users generate pages or images with exponential page inter-arrival intervals (mean equal 60 sec). It is assumed that one page consists of one object, whereas one image consists of five objects. The object size is constant and equal 1000 bytes.

In NRT schemes, the duration of a resource allocation period T has been determined based on the following considerations. First of all, it should be long enough to decrease the number of signalling steps and the number of users simultaneously transmitting the SRs. On the other hand, to preserve the efficiency of resource allocation, T should not exceed the mean inter-arrival time of pages/images in user traffic model (equal 60 sec in our case). Consequently, $T = 10$ slots has been selected.

In all schemes, the target interference levels have been determined based on (39), with $T = 10$ slots and $SINR^{tar} = 0$ dB. Note that the value of T in (39) should be set to be long enough to capture the trending power level for each user. However, because of time-varying wireless channel quality, the observation period should not exceed the fluctuation periodicity of the SINR in time domain. According to a recent study [54], the minimum and mean SINR fluctuation periods (for fixed users operating in outdoor environment) are equal 7 and 25 ms, respectively. Consequently, we can choose any value of T, such that $7 \le T \le 25$.

B. Simulation Results

First, we evaluate the complexity of different algorithms in simulations. Note, that G-RT/NRT use the same formulation

(11) for resource allocation, and therefore their computational complexities are identical. Same is true for 1-RT/NRT and 2-RT/NRT. Figure 4 demonstrates simulation results collected in the network with 10 users in **C**, and the overall number of users N varying from 10 to 150.

Here we observe performance of the proposed algorithms with a so-called "cold" start (denoted G-RT-C, 1-RT-C, 2-RT-C in the figure) and a "warm" start (G-RT-W, 1-RT-W, 2-RT-W). When a "cold" setting is used, we start with initialization $\mathbf{b}^0_{(n)} = \mathbf{c}^0_{(n)} = \mathbf{p}^0_{(n)} = 0$ for any $n \in \mathbf{N}$. In a "warm" setting, we start from the last obtained optimal values of the optimization variables **b**, **c** and **p**. Obtained results show that the "warm" start improves performance of the algorithms in terms of the number of iterations necessary for convergence. Such results can be easily explained by the fact that the external network parameters change more slowly than slot duration (1 ms). Therefore, in general, the "warm" start is much closer to the optimal solution than zero-initialization.

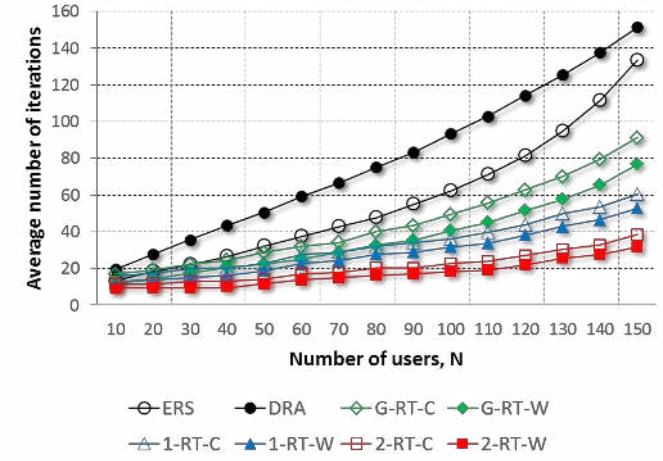

Fig. 4. Average number of iterations necessary for convergence as a function of the overall number of UEs N in simulations conducted for 10 users in **C**.

Let us now evaluate the delay/SINR performance of different schemes in simulations. Figures 5 and 6 illustrate mean packet end-to-end delay and SINR for the network with 10 users in **C**, $N = 110$ and the number of DUs varying from 1 to 99. Figure 5 demonstrates the impact of cellular traffic offloading on mean packet end-to-end delay for UEs. As the number of users operating in D2D mode increases, the packet delay in the network decreases. The speed of decrease in delay is at first (when the number of DUs is less than 50) very fast, and then slows down. A slowing speed of delay increase is explained by decreasing channel quality (see Figure 6 showing the negative impact of increase in the number of DUs on mean SINR).

The graphs on both figures confirm that G-RT/NRT have a superior performance among the proposed algorithms, whereas 2-RT/NRT show the worst service quality. To understand such results, note that in general schemes, DUs and CUs can be allocated both the UL and the DL RBs. On the contrary, in 1-RT/NRT and 2-RT/NRT, the UL RBs are reserved for DUs, and therefore the "choice" of available RBs (and hence the possibility to select the "best" RBs) in these algorithms is more limited compared to G-RT/NRT. Additionally, since the power levels of the users are fixed in 2-RT/NRT, the efficiency of these techniques in terms of reducing the packet delay and achieving the higher SINR levels is diminished. In this regard, the possibility of power allocation in G-RT/NRT and 1-RT/NRT can be considered as an extra degree of freedom in optimization. This degree of freedom, however, results in the growing computational complexity (see Figure 2). Hence, there always exists a trade-off between achieving the best network performance and increased complexity of the algorithm.

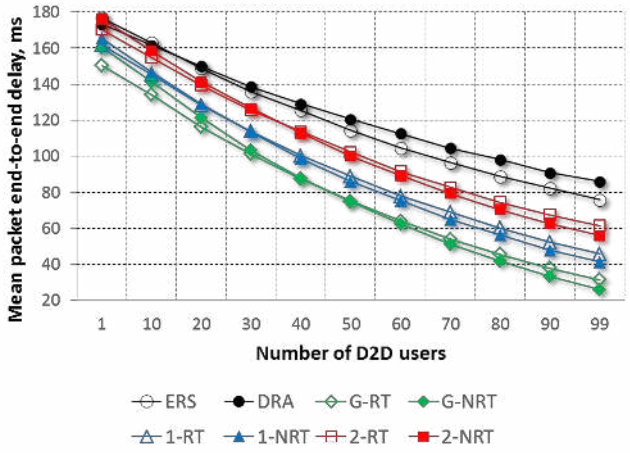

Fig. 5. Mean packet end-to-end delay as a function of the number of UEs operating in D2D mode in simulations conducted for 10 users in **C** and $N = 110$.

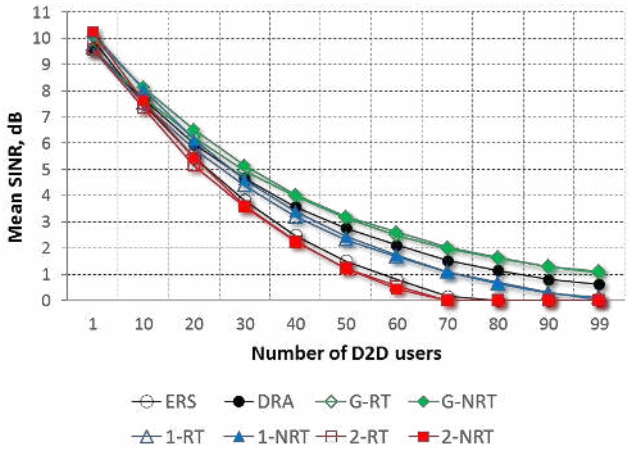

Fig. 6. Mean SINR as a function of the number of UEs operating in D2D mode in simulations conducted for 10 users in **C** and $N = 110$.

Figures 7 and 8 illustrate performance of the network with 10 users in **C** and the overall number of UEs varying from 10 to 150. It follows from these graphs that all NRT schemes achieve slightly better results than the corresponding RT schemes when the number of users is high. Note that if the number of simultaneous SRs in the system is higher than the number of PUCCHs, the UL scheduling delay component is growing, resulting in increased overall packet delay. In NRT, the number of users simultaneously sending SRs is smaller than that in RT procedures, and therefore in highly loaded scenarios, the NRT implementation is more efficient. We also observe that ERS shows the worst performance in terms of mean packet delay. In ERS, the power control, interference management and mode selection are implemented with the objective to minimize the

total transmission power of UEs. This means that this algorithm is originally not designated for improving the QoS (in our case, reducing delay) of the users.

It should be mentioned that all versions of the proposed resource allocation approach show improved (compared to ERS and DRA) delay performance, which can be explained by the use of appropriate objective (buffer size minimization). Note that the objective stated in DRA (PHY-layer sum rate maximization) does not necessarily result in reduced delay for the users. In DRA (and also ERS), the buffer status information is not taken into account. Hence, the allocations according to DRA and ERS algorithms may be very unfair (meaning that the users with lower traffic demands can be allocated more bandwidth then the users with higher traffic demands).

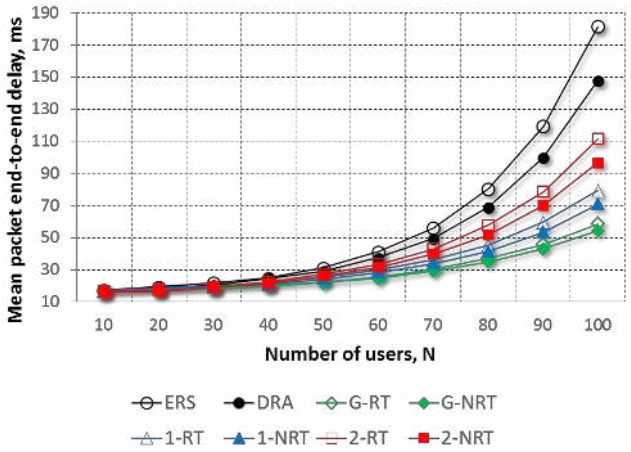

Fig. 7. Mean packet end-to-end delay as a function of overall number of UEs *N* in simulations conducted for 10 users in **C**.

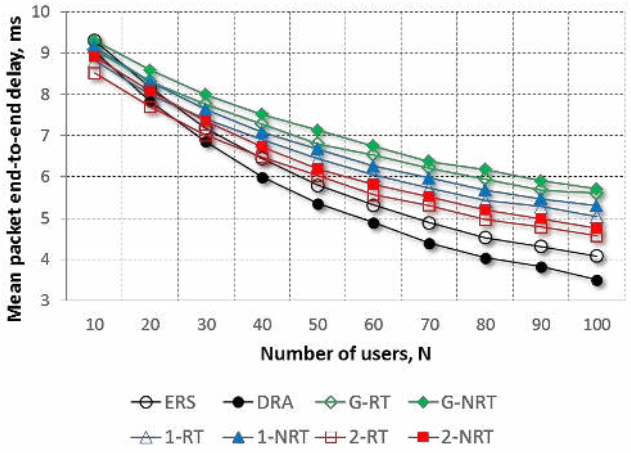

Fig. 8. Mean SINR as a function of the overall number of UEs *N* in simulations conducted for 10 users in **C**.

VII. Conclusion

This paper considers the problem of joint D2D/cellular mode selection, RB allocation, power control and interference management for D2D communication underlaying LTE-A network. The problem has been formulated as an optimization problem where the modes, RBs and power levels of user devices are allocated to maximize the minimum buffer size of UEs subject to certain interference constraints. Possible realizations of a proposed resource allocation approach include general algorithms with real-time and non-real time implementation, as well as the algorithms suitable for LTE-D network (with fixed and controlled power levels of UEs).

Simulation results have shown that all proposed algorithms outperform existing relevant resource allocation schemes in terms of mean packet delay for the users (which is explained by the appropriate choice of optimization objective). General algorithm introduce smaller delay than their LTE-D modifications (the choice of available resources in LTE-D algorithms is limited, since UL RBs are reserved for DUs). The algorithms with the controlled UEs' power levels perform better than the algorithm with fixed UEs' power levels (extra degree of freedom of power assignment provides possibility to obtain more favourable results).

Consequently, to achieve the best results, the number of degrees of freedom (i.e., the number of optimization variables) and the choice of available resources should be as large as possible. However, such widened choice also relates to increase in the size of the problem, resulting in higher complexity of a corresponding algorithm.

References

[1] K. Doppler et.al., "Device-to-device communication as an underlay to LTE-advanced networks," *IEEE Commun. Mag.*, vol. 47, no. 12, pp. 42-49, 2009.

[2] C.-H. Yu et.al., "On the performance of device-to-device underlay communication with simple power control," in *Proc. VTC*, 2009, pp. 1-5.

[3] B. Guo et.al., "Graph-Based Resource Allocation for D2D Communications Underlying Cellular Networks in Multiuser Scenario," *Int. Journal of Antennas and Propagation*, pp. 1 – 6, 2014.

[4] B.-Y. Huang et.al., "Resource Allocation in D2D Communication – A Game Theoretic Approach," in *Proc. ICC*, 2014, pp. 483 – 488.

[5] M. Hasan, E. Hossain, "Distributed Resource Allocation in D2D-Enabled Multi-tier Cellular Networks: An Auction Approach," arXiv preprint arXiv:1501.04199, 2015.

[6] F. Malandrino et.al., "Uplink and Downlink Resource Allocation in D2D-Enabled Heterogeneous Networks," In *Proc. WCNC*, 2014, pp. 87 – 92.

[7] D. Feng et.al., "Device-to-device communications underlaying cellular networks," *IEEE Trans. Commun.*, vol. 61, no. 8, pp. 3541–3551, 2013.

[8] L. Su et.al., "Resource allocation using particle swarm optimization for D2D communication underlay of cellular networks," in *Proc. WCNC*, pp. 129–133, 2013.

[9] Y. Cheng et.al., "Maximum-weight bipartite matching technique and its application in image feature matching," in *Proc. SPIE Conference on Visual Communication and Image Processing*, 1996, pp. 1358–1379.

[10] J. Kennedy, "Particle swarm optimization," in *Encyclopedia of Machine Learning*, 2010, pp. 760–766.

[11] L. Lei et.al., "Operator controlled device-to-device communications in LTE-advanced networks," *IEEE Wireless Commun.*, vol. 19, no. 3, pp. 96 – 104, 2012.

[12] Y Cui et.al., "A Survey on Delay-Aware Resource Control for Wireless Systems – Large Deviation Theory, Stochastic Lyapunov Drift, and Distributed Stochastic Learning," *IEEE Trans. Information Theory*, vol. 58, no. 3, pp 1677 – 1701, 2011.

[13] F. Zhang, V. Lau, "Cross-Layer MIMO Transceiver Optimization for Multimedia Streaming in Interference Networks," *IEEE Trans. Signal Processing*, vol. 62, no. 5, pp. 1235 – 1245, 2014.

[14] A. Asheralieva, K. Mahata, "Resource allocation for LTE-based cognitive radio network with queue stability and interference constraints," *Physical Commun.*, vol. 14, pp. 1 – 13, 2015.

[15] S. Boyd et.al., "Distributed optimization and statistical learning via the alternating direction method of multipliers," *Found. & Trends in Machine Learning*, vol. 3, no. 1, pp. 1 – 122, 2011.

[16] D. P. Bertsekas, J. N. Tsitsiklis, "Parallel and Distributed Computation: Numerical Methods," Athena Scientific, 1997.

[17] H. Wang, A. Banerjee, "Online alternating direction method," arXiv preprint arXiv:1306.3721, 2013.
[18] A. F. T. Martins et.al., "An augmented lagrangian approach to constrained map inference," in *Proc. ICML*, 2011, pp. 169–176.
[19] Q. Fu et.al., "Bethe-ADMM for tree decomposition based parallel map inference," arXiv preprint arXiv:1309.6829, 2013.
[20] P. Scott, S. Thi´ebaux, "Dynamic Optimal Power Flow in Microgrids using the Alternating Direction Method of Multipliers," arXiv preprint arXiv:1410.7868, 2014.
[21] O. Miksik et.al., "Distributed Non-convex ADMM-based inference in large-scale random fields," in *Proc. BMVC*, 2014, pp. 1 – 12.
[22] B. Geibler, "Solving Power-Constrained Gas Transportation Problems using an MIP-based Alternating Direction Method," Tech. report, Friedrich-Alexander-Universität Erlangen-Nürnberg (FAU), 2014, pp. 1 – 25.
[23] H. Holma, A. Toskala, "LTE for UMTS: Evolution to LTE-Advanced," John Wiley and Sons, 2011.
[24] "E-UTRA; MAC protocol specification," 3GPP TS 36.321. (Release 8).
[25] K. Doppler et. al., "Device-to-Device Communication as an Underlay to LTE-Advanced Networks," *IEEE Commun. Mag*., vol. 47, nol. 12, pp. 42 – 49, 2009.
[26] "LTE-Advanced (3GPP Rel.11) Technology Introduction," White Paper, Rohde&Schwarz.
[27] A. Asadi et. al., "A Survey on Device-to-Device Communication in Cellular Networks," accepted for publication in *IEEE Commun. Surveys and Tutorials*, 2014.
[28] D. V. Lindley. "The theory of queues with a single server," *Math. Proc. of the Cambridge Philosophical Society*, vol. 48, no. 2, pp. 277–289, 1952.
[29] P. Mogensen et. al., "LTE Capacity Compared to the Shannon Bound," in *Proc. VTC*, 2007, pp. 1234 – 1238.
[30] "TS 36.300, Evolved Universal Terrestrial Radio Access (EUTRA) and Evolved Universal Terrestrial Radio Access Network (EUTRAN), Rel. 11," 3GPP Tech. Rep., Sep. 2012.
[31] A. Orsino, "Efficient Data Uploading Supported by D2D Communications in LTE-A Systems," arXiv preprint arXiv:1503.09076, 2015.
[32] S.A. Vavasis, "Nonlinear Optimization: Complexity Issues," Oxford University Press, Oxford, 1991.
[33] S.P. Boyd, L. Vandenberghe, "Convex Optimization," Cambridge University Press, 2004.
[34] R. J. Vanderbei, D. F. Shanno, "An interior-point algorithm for nonconvex nonlinear programming," *Comput. Optimization & Applications*, vol. 13, no. 1-3, pp.231-252, 1999.
[35] J. Bolte et.al., "Proximal alternating linearized minimization for nonconvex and nonsmooth problems," *Math. Program*., vol. 146, no. 1-2, pp. 459-494, 2014.
[36] R. Östermark, "Solving a nonlinear non-convex trim loss problem with a genetic hybrid algorithm," *Comput. & Operations Research*, vol. 26, no. 6, pp. 623–635, 1999.
[37] K. Deb, "Multi-objective optimization using evolutionary algorithms," John Wiley & Sons, 2001.
[38] R. Bracewell, "Heaviside's Unit Step Function, H(x)," *The Fourier Transform and Its Applications, 3d ed*. New York: McGraw-Hill, 2000, pp. 61-65.
[39] M. Ó. Searcóid, "Metric spaces," *Springer undergraduate mathematics series*, Berlin, New York: Springer-Verlag, 2006.
[40] L. Xiao and S. Boyd, "Fast Linear Iterations for Distributed Averaging," *Systems and Control Letters*, vol. 53, pp. 65-78, 2004.
[41] R. Kannan, C. Monma, "On the computational complexity of integer programming problems," in *Optimization and Operations Research*, 157, Lecture Notes in Economics and Math. Systems, 1978, pp. 161-172.
[42] S. Leyffer, "Integrating SQP and branch-and-bound for mixed integer nonlinear programming," *Comput. Optimization & Applications*, vol. 18, pp. 295 – 309, 2001.
[43] L. Liberti, N. Mladenovic, G. Nannicini, "A good recipe for solving MINLPs," in *Hybridizing metaheuristics and math. program*., 10, Annals of Inform. Systems, 2009, pp. 231–244.
[44] G. Nannicini, P. Belotti, "Local branching for minlps," Tech. Report Working paper, CMU, 2009.
[45] T. Berthold, "Heuristic algorithms in global MINLP solvers," Verlag Dr. Hut, 2014.
[46] C. D'Ambrosio et. al., "A storm of feasibility pumps for nonconvex MINLP," *Math. Program*., vol. 136, no. 2, pp. 375-402, 2012.
[47] M. Fischetti, D. Salvagnin, "Feasibility Pump 2.0," *Math. Program*., vol. 1, no. 2-3, pp. 201 - 222, 2009.
[48] S. Burer, A. N. Letchford, "Non-convex mixed-integer nonlinear programming: A survey," *Surveys in Operations Research and Manag. Science*, vol. 17, pp. 97 - 106, 2012.
[49] Overview of 3GPP Release 12. V0.1.4, September 2014.
[50] A. Asheralieva, K. Mahata, J. Y. Khan, "Delay Aware Resource Allocation Scheme for a Cognitive LTE Based Radio Network," in *Proc. MASS*, 2014, pp. 242 – 246.
[51] OPNET. Available online: http://www.opnet.com
[52] D. Wu et.al., "Energy-Efficient Resource Sharing for Mobile Device-to-Device Multimedia Communications," *IEEE Trans. Vehic. Tech*., vol. 63, no. 5, pp. 2093 – 2103, 2014.
[53] IPOGUE, Internet study 2007 and 2008/2009, research report.
[54] C. Lameiro et.al., "Experimental Evaluation of Interference Alignment for Broadband WLAN Systems," arXiv preprint arXiv:1309.4355, 2015.